Journal of Composite Materials

Effects of voids on quasi-static and tension fatigue behaviour of carbon-fibre composite laminates

Sanjay Sisodia, E Kristofer Gamstedt, Fredrik Edgren and Janis Varna

The online version of this article can be found at:
http://jcm.sagepub.com/content/early/2014/07/03/0021998314541993

Effects of voids on quasi-static and tension fatigue behaviour of carbon-fibre composite laminates

Sanjay Sisodia[1,2], E Kristofer Gamstedt[1], Fredrik Edgren[2] and Janis Varna[3]

Abstract

The effect of voids on quasi-isotropic carbon-fibre reinforced plastic laminates under quasi-static loading is compared with that under cyclic tension loading. Emphasis is placed on following damage development at the non-crimp fabric ply-level by investigating the influence of voids on damage accumulation, most notably transverse cracking and delamination. Details from experiments include micrographs of voids taken in both scanning-electron and light microscopy, measurements of void content and crack density using light microscopy, and stiffness plots from both quasi-static and cyclic tests. The stiffness results are compared with theoretical predictions accounting for transverse cracks. Voids have a significantly more detrimental effect on the mechanical properties in cyclic loading compared with quasi-static loading. Specifically, the stiffness reduction development, the underlying transverse cracking in layers and the number of cycles to failure are affected. Quality control by only quasi-static testing for void-containing composite materials to be used in components subjected to fatigue cannot therefore be recommended.

Introduction

In recent years, resin-transfer moulded (RTM) carbon-fibre composites have gained interest as a cost-efficient alternative to autoclave cured composites. Although the quality of RTM composites has improved significantly, the resin flow in the manufacturing step inevitably induces some degree of voids in the material, which cannot be found in autoclave-manufactured composites. In higher end applications, fatigue resistance is a desired property. The effects of voids on fatigue behaviour have been studied in Lambert et al.,[1] Bureau and Denault,[2] de Almeida and dos Santos Nogueira Neto,[3] Chambers et al.[4] and Rotem and Nelson.[5] This study focuses on the effects of voids on fatigue and static properties of carbon fibre reinforced plastic laminates.

Material evaluation is increasingly oriented towards understanding variability of the material properties and investigating reasons for material failure.[1,6–9] The constituent materials of the composites, the fibre–matrix interface, the fibre architecture and microstructural inhomogeneity play an important role in the fatigue performance.[9] In RTM manufactured composites, the thermoset matrix contain voids. When voids are present (see Figure 1), the overall matrix behaviour of the final composite are not well known. This article explores the previous studies and discusses the results from present experiments. A comparison is made between the effects of voids on static and fatigue behaviour, respectively.

Defects like voids are regarded as being inherent in manufacturing techniques such as RTM which is well described in the literature.[10–13] Voids may act as local stress concentrators and reduce the delamination

[1]Department of Engineering Sciences, Division of Applied Mechanics, Uppsala University, Uppsala, Sweden
[2]GKN Aerospace, Trollhättan, Sweden
[3]Department of Engineering Sciences and Mathematics, Division of Materials Science, Luleå University of Technology, Luleå, Sweden

Corresponding author:
Sanjay Sisodia, Department of Engineering Sciences, Division of Applied Mechanics, Uppsala University, SE-75121 Uppsala, Sweden.
Email: sanjay.sisodia@angstrom.uu.se
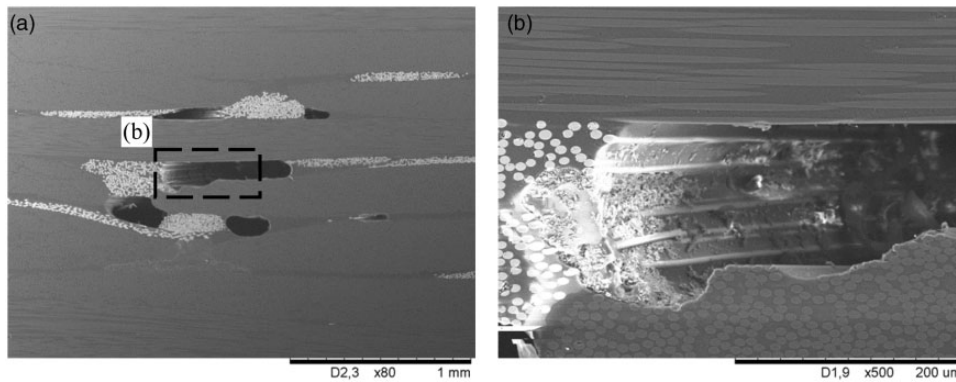
Figure 1. Scanning-electron micrograph of a polished cross-section showing (a) voids in a non-crimp fabric reinforced epoxy composite and (b) an enlarged view of the indicated void.

resistance,[13–15,2,16,17,3,18–20] compression strength,[13,21] shear strength,[13–15,2,16,21–25] various bending properties[13–15,16,17,3,22,26,27] and fatigue strength.[13,2–5]

Experimental micromechanical studies allow to better understand the underlying mechanisms and the weak link in the material microstructure.[28] As an example, Prakash[29] used scanning-electron microscopy and ultrasonic methods during progressive fatigue loading to study fibre debonding as controllable parameter, which, in turn, led to the selection of what Ashby and Bréchet[28] describe as selection of a proper matrix material. Related studies on the effects of interface properties have also been done in Lambert et al.,[1] Hapke et al.[30] and Kosek and Sejak.[31] In a similar spirit, we focus in this study on the damage mechanisms induced by the presence of voids in cyclic loading. This has been done by investigating the stiffness and damage accumulation in tension and cyclic loading for two void concentrations, namely 0.8% and 3%. Furthermore, the void content was varied systematically to see the effects in cyclic loading. For all tests, a multidirectional laminate with quasi-isotropic layup was examined. For the assessment of void content and crack density, optical microscopy and replication techniques have proven to be adequate. Results from experiment are also compared with theoretical predictions based on models accounting for transverse cracking in layers[32–35] and the ply-discount model in the framework of classical laminate theory (CLT).

Experimental procedures

Materials

Composite laminates were manufactured through RTM to produce a low and controlled level of volume voids as described in George and Drechsler.[12] The composite reinforcement was a carbon fibre (HTS40) uni-directional (UD) non-crimp fabric with

Table 1. Experimentally characterised elastic constants of unidirectional plies at 25°C (0.8% voids).[a]

Modulus	GPa
Tension − 0°, E_1	126.60
Tension − 90°, E_2	9.18
In-plane shear, G_{12}	3.90
Poisson's ratio, v_{12}	0.31

[a]The values are used in the stiffness predictions of the damaged laminates.

fibre areal weight of 242.5 g/m². Quasi-isotropic lay-ups of the reinforcement were prepared for laminate production using 16 layers. The laminate stacking sequence was $[0/-45/90/+45]_{2s}$. The resin used was Hexcel's HexFlow RTM6.

For the purpose of obtaining high concentration voids in the material, sample laminates were manufactured with the same materials, but with a wet layup process. This process entailed pouring the resin onto the mould, then laying the reinforcement on top, sealing it with a semi-permeable membrane, and applying vacuum across the top of the membrane. The mould and resin were pre-heated to 80°C. To induce a high level of volume voids, the resin was vigorously stirred for several minutes to aerate it. A vacuum pressure of 60 mbar was applied above the membrane, and then the mould was placed into an oven to start a standard RTM6 cure.

The resulting fibre volume fraction for all laminates ranged from 53.6% to 56.0%. Experimentally characterised elastic constants for unidirectional plies are given in Table 1. From the produced plates, samples with dimensions 175 × 25 × 4 mm were cut using a diamond saw. The thickness of an individual ply was 0.25 mm. End tabs were made of glass fibre/epoxy material with dimensions 40 × 25 × 1.5 mm, and were

bonded on the specimen using a two component epoxy adhesive system (Araldite AW4858). The gauge length between the tabs was 90 mm. Sample dimensions are based on details from Sisodia et al.[36] and ASTM.[37]

Image analysis

The specimens for image analysis were prepared using silicon carbide abrasive paper, and final polish was applied using synthetic diamond compound of 0.25 μm. A light microscope with a digital camera was used to examine the specimens. Preliminary work established a magnification of ×500 and five images per specimen provided statistically representative data for reliable void content characterisation. The images were captured using Leica Application Suite and analysed using MATLAB's Image Processing Toolbox. The analysis provided a quantification of void content, denoted by V_V, with respect to the total volume of the composite including the three components fibres, matrix and voids. Some example images of unloaded laminates are shown in Figure 2.

Quasi-static loading

Quasi-static tests were initially done in an Instron 4505 mechanical testing machine to obtain the stress–strain relationship and determine the stiffness and crack density after loading to given strain values. Tests were performed under displacement control using a crosshead speed of 1 mm min^{-1} in dry conditions at 25°C. The specimens were loaded and unloaded to increasing levels of strain using fixed increments of strain. Between each ramp, a hold time of 5 min was implemented to allow for relaxation. For strain measurements, an extensometer Instron 2620-602 with a gauge length of 50 mm was used. Before unloading, edge replicas of the specimen were taken to determine the density of transverse cracks. In this manner, the laminate stiffness and the corresponding crack density was found after each load increment. The elastic modulus was obtained as linear trendline for all data points along the unloading slope, between 0.1% and 0.3% strain. The average longitudinal modulus for three undamaged specimens was 46 GPa. This compares well with the analytical approximation 48 GPa when using CLT and the elastic properties of the individual plies in Table 1.

Cyclic loading

Fatigue tests were carried out in a 100 kN servo-hydraulic Schenk PB250 mechanical testing machine with a ±25 mm potentiometer to trace the crosshead
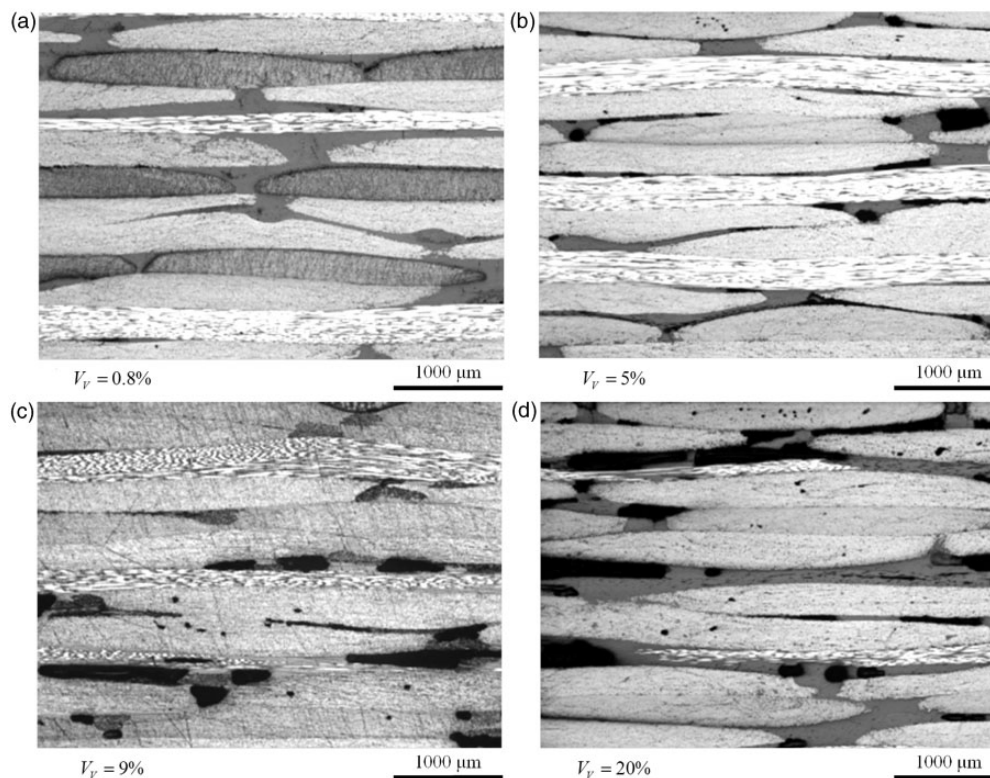
Figure 2. Light microscope images of laminates with voids.

motion. The cyclic tests were performed under load control at a frequency of 7 Hz and a load ratio of $R = 0.1$ in dry conditions at 25°C. The applied maximum stress in cyclic loading was 370 MPa. This corresponded to 60% of the ultimate strength or 0.8% strain in quasi-static loading for a laminate with 0.8% voids. This stress level assured a low risk for run-outs and too few cycles to failure with a static-like failure. Failure in fatigue was defined as total loss of laminate load carrying capability. The elastic modulus in fatigue testing was determined by dividing the difference between the maximum and minimum applied stresses by the difference between the maximum and minimum strains.

Crack quantification

It is not self-evident that the crack-density data for the specimen edges is representative of the damage state inside the specimen. Especially in fatigue of thin layer laminates it may happen that the tunnelling cracks are initiated at the specimen edges but they do not grow at once over the whole width of the specimen.[38] As a consequence, the crack density measured by edge observations may be higher than the average value over the whole volume of the lamina. A uniformity check of the crack-density distribution across the width of the laminate sample was done for both the quasi-static and cyclic tests. In the quasi-static case damage was characterised on the specimen edges and in a section at specimen centre width after loading to 1% applied strain. A similar cutting and inspection procedure was done in fatigue. It should also be noted that crack densities measured in the 45-layers are averaged readings for the entire laminate.

In quasi-static tests, a surface replication technique was used for in situ determination of microstructural deterioration and damage accumulation of the material. Surface replicas provided an image of the surface topography of the polished edge of the specimen. Replicas were produced using Repliset T1 by Struers. The compound was applied and extracted before unloading. After the last strain increment, the test samples were studied under the microscope to confirm that the crack density evolved uniformly through the laminate width and that edge view is representative for the damage state in the laminate. Samples were cut in the axial direction at about 50% of the width. This resulted in four surfaces for study under the microscope, namely two internal surfaces from the axial split and the two opposite edges of the laminate. After cyclic loading, the samples were cut in the axial direction and the created surfaces were inspected for cracks using light microscopy.

Results and discussion

### Effects of voids on mechanical properties

Three categories of material properties have been subject to measurement and analysis in experiments. One has been referred to as fatigue life (i.e. number of load cycles to final failure). The other two properties are quasi-static strength and stiffness, and are expressed in terms of the elastic modulus obtained from quasi-static stress–strain curves. For these three properties, all related data points were normalised with the corresponding value at 0.8% voids, which corresponds to the technically void-free material. Using the RTM technique, it was not possible to produce totally void free laminates (i.e. 0% voids). A total of 28 samples were used to produce the results presented in Figure 3; 24 samples for fatigue loading and 4 samples for static loading. All data have been fitted by least squares with power law trend lines, rendering linear relations in log–log plots. There is negligible influence of the voids on the quasi-static strength and stiffness. There is no significant difference in quasi-static properties for laminates with 0.8–5% voids. For the same increase in void content, the fatigue life degrades by two orders of magnitudes, and for laminates up to 20% voids by three orders of magnitudes. Although it should be kept in mind that fatigue life and static tensile parameters are quite different properties, there is clearly a striking difference in void sensitivity on these fatigue and static mechanical properties. Both fatigue life and tensile properties are parameters used in design or materials selection, and can be compared if normalised as in Figure 3.

Material properties for two void concentrations

Crack-density distribution. Measurements of crack density were done in both quasi-static and fatigue loading. Results in Figure 4(a,b) for quasi-static loading after 1% strain show that crack densities on specimen edges and in specimen centre are consistent, and that the deviations do not have any systematic trend, which suggest that edge measurements are representative. For cyclic loading, samples were loaded for duration of 1000 cycles and then sectioned for fracture study (Figure 4c,d). One sample for each respective load case is presented in Figure 4. The conclusion is that damage in the centre of the specimen is the same as observed on the edge. In the quasi-static test at 1% strain the laminate voids has no noticeable effect on the crack density in the 45°-layers. The effect of voids is larger on cracking in the 90°-layer. In cyclic loading similar trends can be observed. A more brittle and void-sensitive formation of transverse cracks is expected in the 90° plies. The significant shear stresses in the
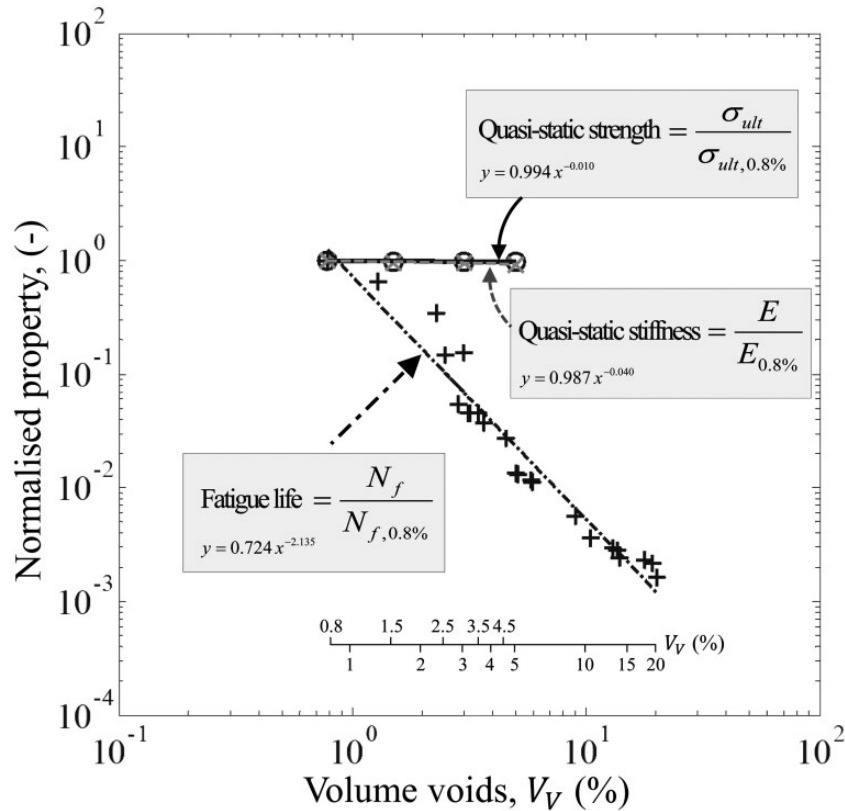
Figure 3. Normalised engineering properties plotted against volume voids: quasi-static strength and stiffness normalised with that for a technically void-free laminate ($V_V = 0.8\%$), and fatigue life at a maximum stress level of 60% of the ultimate tensile strength normalised with the corresponding fatigue life for a void-free laminate.
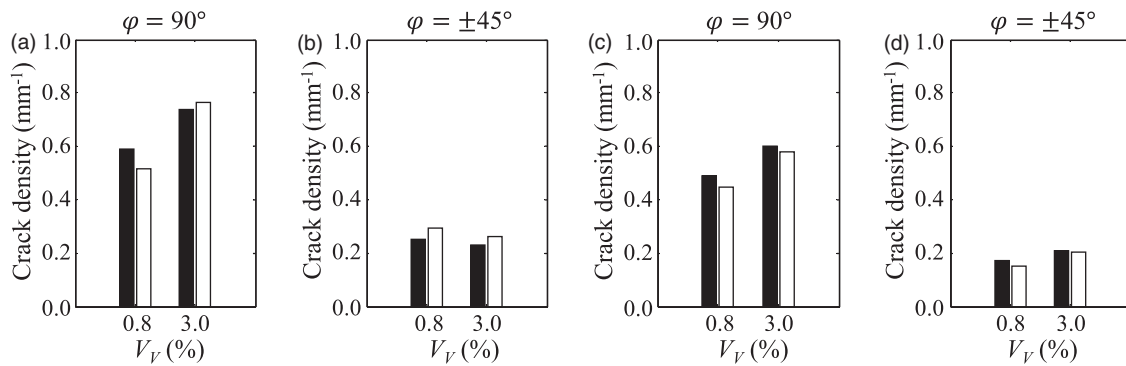

Figure 4. Uniformity check for crack density in laminate with voids (V_V) (■ at edge, □ at ~50% width): (a,b) quasi-static test at 1% applied strain; and (c,d) cyclic test at $N = 1000$ cycles and 60% of the ultimate tensile strength.

polymer matrix in the 45° plies generally make deformation non-linear, more ductile and the crack formation becomes less sensitive to flaws.[39,40]

Quasi-static properties. Axial modulus reduction as a function of increasing applied strain was measured for two laminates with voids at 0.8% and 3%. The axial modulus E was normalised with respect to the initial

specimen modulus without any transverse cracks E_0. The typical behaviour of one specimen for each void concentration is presented in Figure 5. The normalised stiffness E/E_0 is plotted along the ordinate in Figure 5(a). The experimental results for crack density versus applied strain are presented in Figure 5(b).

Cracking in the 90° plies starts at strains above 0.3%, as can be seen in Figure 5(b). A distinct
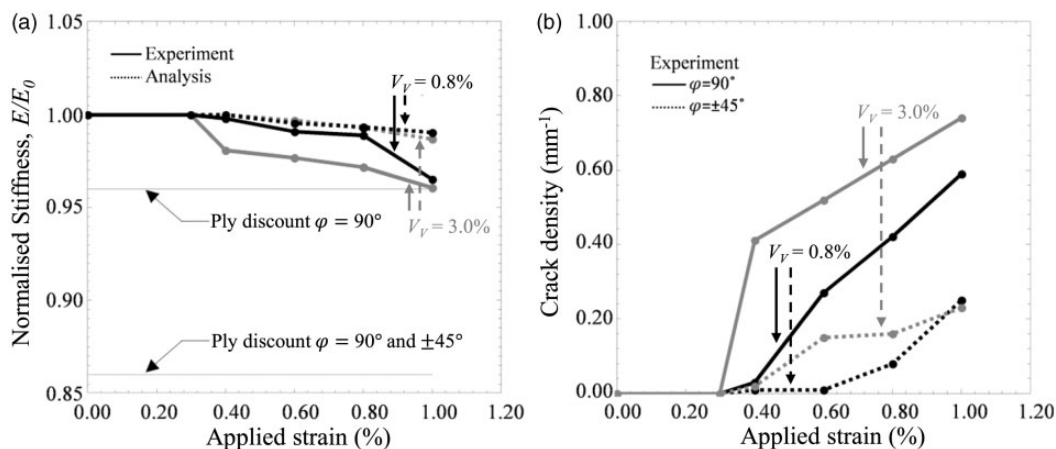
Figure 5. Effects of voids on quasi-static material properties. Stiffness retention normalised with the initial modulus for the undamaged laminate.

difference is seen in crack density already at 0.4% strain, where the laminate with 3% voids has extensive cracking and stiffness drops by 2% (Figure 5a); whereas the 0.8% voids show very little signs of damage or stiffness change. At intermediate strains the cracking in the 90° plies increases in both laminates but in the laminate with high voids even the 45° plies starts to crack. The stiffness decrease does not show the same trend. At 1% strain, both laminates are showing almost the same crack densities in both the 90° and the 45° plies, and also the same stiffness decreases. It seems, thus, that voids have an effect on the initiation of micro cracks and not on the saturated crack density for the present material. However, this may not be the general case, since other types of composites may be affected differently by the degree of local stress relaxation due to different kinds of damage and viscous deformation.

These trends (Figure 5a,b) are related to the statistical nature of the transverse cracking process in the specimen and the size and spatial distribution of voids.[21] Defects located at random positions in each layer cause the weakest link to fail first. Eventually, the ply will be saturated with transverse cracks, since build-up of sufficiently high stresses to cause further cracking between existing cracks is no longer possible. This explains the commonly observed sigmoidal of the crack density curve.[35] The voids are distributed statistically (size and location) creating regions of local stress concentration on loading. In regions with a high density of sufficiently large voids, transverse cracking starts earlier, usually connecting voids, as shown in Figure 6. This explains the sensitivity of the crack density to void content in the low strain region. With increasing applied strain the multiple cracking continues primarily in locations containing voids. After cracks have developed in all local concentration zones, further cracking is possible only in regions with no voids. This may be

the reason why the crack density at high strain becomes less dependent on the void content, as observed in Figure 5(a,b).[34] For static stiffness design of RTM-manufactured laminates, it is therefore advisable to control the processing conditions so that the transverse-crack inducing voids are on average further apart than the transverse-crack density at saturation.

In Figure 5(a), two model predictions are presented, viz. the ply-discount model and the analytical global-local model are presented in Appendix 1. The ply-discount model here represents the extreme case of zero stiffness in the transverse and shear directions for the plies containing transverse cracks (here the 90° plies, or both the 90° and ±45° plies). The more detailed analytical model depends on crack densities and accounts for realistic stress transfer between transverse cracks. As expected, the ply-discount model underestimates the stiffness, which can be explained by that cracked plies still carry load. The analytical model predicts stiffness relatively close to the measured values. In this case, the stiffness is slightly overestimated. A possible reason is that the model does not account for delaminations. Even under static conditions, small interply delamination can be observed, starting to form where the transverse cracks intersect with the adjacent plies. However, for low stresses and not too high number of elapsed load cycles, the model predicts the stiffness change accurately.

Fatigue properties. Figure 7 shows stiffness retention and crack density versus number of cycles for two laminates with voids at 0.8% and 3%. The highest density of cracks can be found, as expected, in the 90° layer. The presence of voids accelerates the cracking and at low number of cycles. Many more cracks are present in layers of laminate with high voids (as was also observed for intermediate strains in the quasi-static case, cf. Figure 5). With increasing number of cycles the
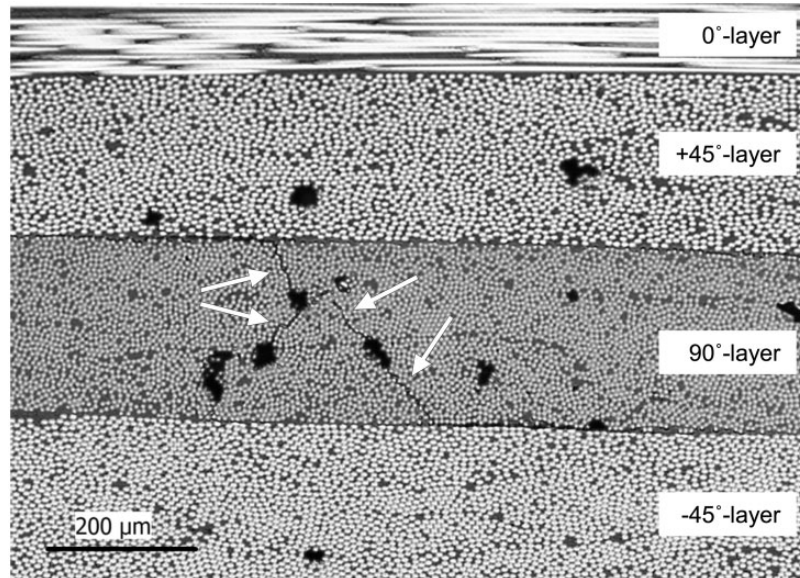
Figure 6. Arrows indicate transverse cracks which connect voids in 90°-layer at 0.4% strain in quasi-static loading of laminate with $V_V = 3\%$.
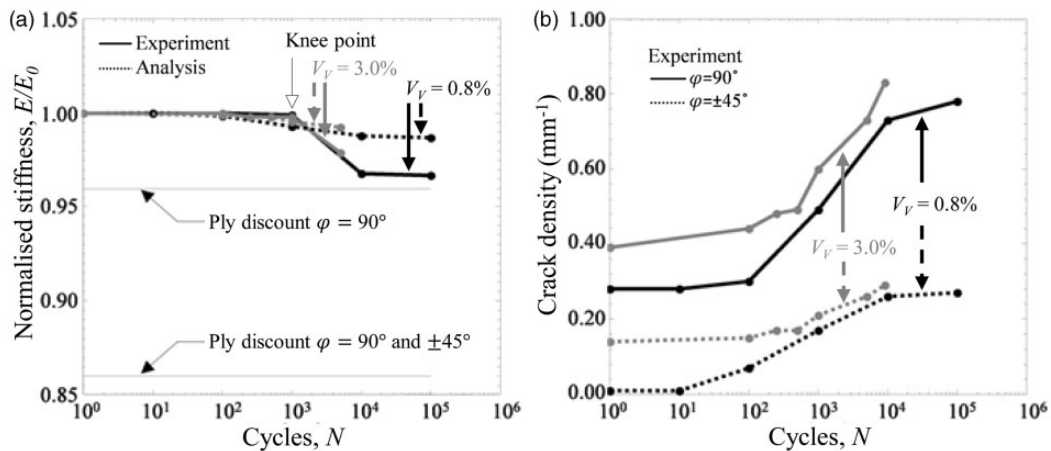

Figure 7. Effects of voids on fatigue material properties. Stiffness retention is normalised to first cycle modulus (i.e. E/E_0).

cracking continues and the effect of the presence of voids on it becomes smaller and smaller, cf. Figure 5(b). The same tendency was observed for increasing strain under quasi-static conditions. It could be assumed that when transverse cracking approaches saturation, both under quasi-static and cyclic conditions, the remaining uncracked ply segments between transverse cracks are void free, or that the small voids therein are not sufficiently large to cause any further cracking.

As can be noticed in Figure 7(a), the ply-discount model severely underestimates the stiffness, since it here assumes that cracked plies carry no transverse or shear stresses. The results for crack densities in each layer

were used in the analytical model to calculate the elastic modulus reduction for the laminate at each experimentally determined damage. During the first 1000 cycles the difference in normalised modulus between the analytical predictions and experiments is very small (0–0.5%). After 1000 cycles the predictions are systematically greater than the experimentally measured. The differences with experiment become greater at higher number of cycles. It may be explained by the observed delaminations that are not included in the model. Delaminations have been known to grow progressively during fatigue, and emanate from transverse crack tips.[41] The main reason for the stiffness decrease is the underlying accumulation of transverse cracks and
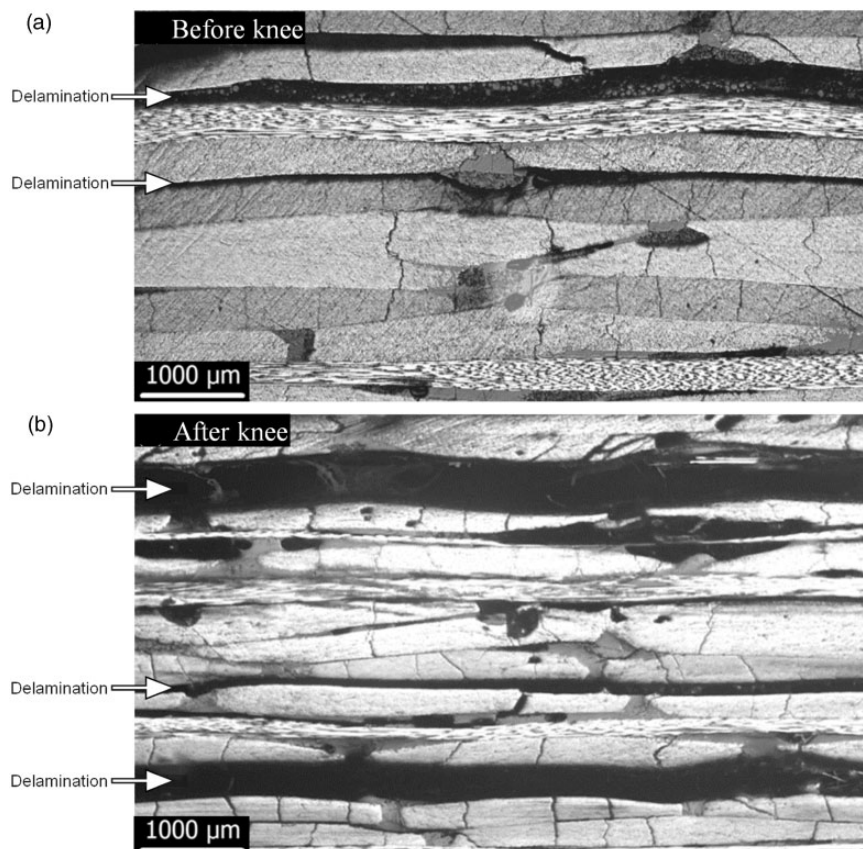
Figure 8. Fatigue damage at $R = +0.1$ for laminate with $V_V = 3\%$, particularly at (a) 10,000 cycles and (b) 100,000 cycles.

is shown to increase progressively during fatigue, cf. Figure 7(b).

Figure 8 shows the fracture morphology of a laminate with 3% voids before and after the 'knee', which can be seen in Figure 7(a). Before the knee point the stiffness is almost constant during cyclic loading. At some point, the stiffness starts decreasing noticeably during continued fatigue. This defines the knee point for stiffness degradation in cyclic loading. The controlling mechanism for this distinct drop in stiffness is gross delamination. As can be seen in Figure 8, before the knee point, the delaminations are limited. After this point, the delaminations have spread to most load carrying plies of the laminate. Full delamination means that loads cannot be transferred from one ply to another, and the load-carrying capacity is entirely lost in the fully delaminated ply. Eventually, it is the 0° plies that carry all loads, which essentially is the critical ply controlling the residual fatigue life after failure and delamination of the all other off-axis plies.[42,43]

Conclusions

This study has been investigating the effect of voids on quasi-isotropic laminates under cyclic tensile loading and quasi-static tensile loading. The following conclusions can be made:

- The fatigue life of the investigated carbon-fibre reinforced plastic laminates was found to be very sensitive to the void concentration, induced from the resin impregnation process. In comparison to this void sensitivity on fatigue behaviour, the effects of voids on quasi-static strength and stiffness are negligible. In light of this marked difference in void sensitivity, it should be emphasised that only quasi-static mechanical testing is not sufficient in quality control of composite materials intended for components to be used under fatigue conditions.
- The sensitivity to voids was found to be greater for transverse cracking in the 90° plies than in off-axis plies, both under cyclic and quasi-static conditions. The sensitivity is most significant at intermediate static strains and during multiplication of transverse cracking in fatigue.
- The measured stiffness was compared with predictions from the ply-discount model and an analytical global-local model accounting for the measured transverse crack densities. The ply-discount model significantly underestimates the stiffness, since it

assumes that plies with cracks do not carry any load. The analytical model slightly overestimates the stiffness. This difference becomes significant after extended fatigue or at high static strains. The laminates then contain a considerable amount of delaminations. The deviance between the model and the experimental results indicate the onset of extensive delamination.

- Plots of the stiffness retention as a function of the number of load cycles typically show two distinct regimes; one with constant stiffness during the first part of the fatigue life, and after a knee point, a monotonic drop in stiffness. Microscopic investigations show that before the knee point delaminations between the cracked plies remain limited, but after this point there is substantial overall delamination.

Conflict of interest

None declared.

References

1. Lambert J, Chambers AR, Sinclair I, et al. 3D damage characterisation and the role of voids in the fatigue of wind turbine blade materials. *Compos Sci Technol* 2012; 72: 337–343.
2. Bureau MN and Denault J. Fatigue resistance of continuous glass fiber & polypropylene composites: consolidation dependence. *Compos Sci Technol* 2004; 64: 1785–1794.
3. de Almeida SFM and dos Santos Nogueira Neto Z. Effect of void content on the strength of composite laminates. *Compos Struct* 1994; 28: 139–148.
4. Chambers AR, Earl JS, Squires CS, et al. The effect of voids on the flexural fatigue performance of unidirectional carbon fibre composites developed for wind turbine applications. *Int J Fatigue* 2005; 28: 1389–1398.
5. Rotem A and Nelson HG. Failure of a laminated composite under tension-compression fatigue loading. *Compos Sci Technol* 1989; 36: 45–62.
6. Gagel A, Fiedler B and Schulte K. On modelling the mechanical degradation of fatigue loaded glass-fibre non-crimp fabric reinforced epoxy laminates. *Compos Sci Technol* 2006; 66: 657–664.
7. Adden S and Horst P. Stiffness degradation under fatigue in multiaxially loaded non-crimped-fabrics. *Int J Fatigue* 2010; 32: 108–122.
8. Rheinfurth M, Kosmann N, Sauer D, et al. Lamb waves for non-contact fatigue state evaluation of composites under various mechanical loading conditions. *Compos Part A* 2012; 43: 1203–1211.
9. Vallons K, Adolphs G, Lucas G, et al. Quasi-UD glass fibre NCF composites for wind energy applications: a review of requirements and existing fatigue data for blade materials. *Mech Ind* 2013; 14: 175–189.
10. Gehrig F, Mannov E and Schulte K. Degradation of NCF-epoxy composites containing voids. In: *17th international conference on composite materials*, The British Composites Society, Edinburgh, United Kingdom, 2009.
11. Ruiz E, Achim V, Soukane S, et al. Optimization of injection flow rate to minimize micro/macro-voids formation in resin transfer molder composites. *Compos Sci Technol* 2006; 66: 475–486.
12. George A and Drechsler K. Void characterization and membrane selection in the vacuum assisted process. In: *15th European conference on composite materials*, Venice, Italy, 2012.
13. Fiedler B and Schulte K. Reliability and life prediction of composite structures. *Compos Sci Technol* 2006; 66: 615.
14. Guo ZS, Liu L, Zhang BM, et al. Critical void content for thermoset composite laminates. *J Compos Mater* 2009; 43: 1775–1790.
15. Zhang A and Zhang D. The mechanical property of CFRP laminates with voids. *Adv Mater Res* 2013; 652–654: 25–28.
16. Liu L, Zhang BM, Wang DF, et al. Effects of cure cycles on void content and mechanical properties of composite laminates. *Compos Struct* 2006; 73: 303–309.
17. Koissin V, Kustermans J, Lomov SV, et al. Structurally stitched NCF preforms: quasi-static response. *Compos Sci Technol* 2009; 69: 2701–2710.
18. Naganuma T, Naito K, Kyono J, et al. Influence of prepreg conditions on the void occurrence and tensile properties of woven glass fiber-reinforced polyimide composites. *Compos Sci Technol* 2009; 29: 2428–2433.
19. Varna J, Joffe R, Berglund LA, et al. Effect of voids on failure mechanisms in RTM laminates. *Compos Sci Technol* 1995; 52: 241–249.
20. Zhu H, Wu B, Li D, et al. Influence of voids on the tensile performance of carbon/epoxy fabric laminates. *J Mater Sci Technol* 2011; 27: 69–73.
21. Costa ML, Rezende MC and de Almeia SFM. Strength of hygrothermally conditioned polymer composites with voids. *J Compos Mater* 2005; 39: 1943–1961.
22. Chambers AR, Earl JS, Squires CS, et al. Porosity reduction using optimized flow velocity in resin transfer molding. *Compos Part A* 2008; 39: 1859–1868.
23. Zhu HY, Li DH, Zhang DX, et al. Influence of voids on interlaminar shear strength of carbon/epoxy fabric laminates. *Trans Nonferrous Metals Soc China* 2009; 19: 470–475.
24. Thomason JL. The interface region in glass fibre-reinforced epoxy resin composites: 1. Sample

preparation, void content and interfacial strength. *Composites* 1995; 26: 478–498.

25. Costa ML, de Almedia SFM and Rezende MC. The influence of porosity on the interlaminar shear strength of carbon/epoxy and carbon/bismaleimide fabric laminates. *Compos Sci Technol* 2001; 61: 2101–2108.

26. Hagstrand PO, Bonjour F and Månson JAE. The influence of void content on the structural flexural performance of unidirectional glass reinforced polypropylene composites. *Compos Part A* 2005; 36: 705–714.

27. Wisnom MR, Reynolds T and Gwilliam N. Reduction in interlaminar shear strength by discrete and distributed voids. *Compos Sci Technol* 1996; 56: 93–101.

28. Ashby MF and Bréchet YJM. Designing hybrid materials. *Acta Mater* 2003; 51: 5801–5821.

29. Prakash R. Significance of defects in the fatigue failure of carbon fibre reinforced plastics. *Fibre Sci Technol* 1981; 14: 171–181.

30. Hapke J, Gehrig F, Huber N, et al. Compressive failure of UD-CFRP containing void defects: in situ SEM microanalysis. *Compos Sci Technol* 2011; 71: 1242–1249.

31. Kosek M and Sejak P. Visualization of voids in actual C/C woven composite structure. *Compos Sci Technol* 2009; 69: 1465–1469.

32. Lundmark P and Varna J. Constitutive relationships for laminates with ply cracks in in-plane loading. *Int J Damage Mech* 2005; 14: 235–261.

33. Lundmark P and Varna J. Crack face sliding effect on stiffness of laminates with ply cracks. *Compos Sci Technol* 2006; 66: 1444–1454.

34. Varna J. Modeling mechanical performance of damaged laminates. *J Compos Mater* 2013; 47: 2443–2474.

35. Lundmark P and Varna J. Stiffness reduction in laminates at high intralaminar crack density: effect of crack interaction. *Int J Damage Mech* 2011; 20: 279–297.

36. Sisodia S, Kazemahvazi S, Zenkert D, et al. Fatigue of composites with in-situ full-field strain measurements. In: *18th international conference on composite materials*, The Korean society of composite materials, Jeju Island, South Korea, 2011.

37. ASTM. D3039/D3039M – 08 standard test method for tensile properties of polymer matrix composite materials. ASTM International, 2014.

38. Berthelot JM. Transverse cracking and delamination in cross-ply glass-fiber and carbon-fiber reinforced plastic laminates: static and fatigue loading. *Appl Mech* 2003; 56: 111–147.

39. Varna J, Joffe R, Akshantala NV, et al. Damage in composite laminates with off-axis plies. *Compos Sci Technol* 1999; 59: 2139–2147.

40. Pettersson KB, Neumeister JM, Gamstedt EK, et al. Stiffness reduction, creep, and irreversible strain in fiber composites tested in repeated interlaminar shear. *Compos Struct* 2006; 76: 151–161.

41. Gamstedt EK and Sjögren BA. An experimental investigation of the sequence effect in block amplitude loading of cross-ply composite laminates. *Int J Fatigue* 2002; 24: 437–446.

42. Jamison RD, Schulte K, Reifsnider KL, et al. Characterization and analysis of damage mechanisms in tension-tension fatigue of graphite/epoxy laminates. In: *Effects of defects in composite materials, ASTM STP 836*, American Society for Testing and Materials, 1984, pp.21–55.

43. Gamstedt EK and Talreja R. Fatigue damage mechanisms in unidirectional carbon-fibre-reinforced plastics. *J Mater Sci* 1999; 34: 2535–2546.

44. Loukil MS, Varna J and Ayadi Z. Engineering expressions for thermo-elastic constants of laminates with high density of transverse cracks. *Compos Part A* 2013; 48: 37–46.

45. Yongxin H, Varna J and Talreja R. Processing and fabrication of advanced materials – XIX. In: Bhattacharyya D, Lin R and Srivatsan T (Eds) *The Effect of Manufacturing Quality on Transverse Cracking in Cross Ply Laminates*. Auckland, University of Auckland, 2011, pp.552–559.

Appendix 1

Analytical stiffness model

In an attempt to understand the observed laminate stiffness reduction during the loading, experimental data were compared with theoretical predictions based on models accounting for transverse cracking in layers. The model considers a symmetric N-layered laminate. The k-th layer of the laminate is characterised by thickness t_k and fibre orientation angle θ_k. Direction 1 is fibre direction in the layer and direction 2 is transverse to fibres. The total laminate thickness is denoted h,

$$h = \sum_{k=1}^{N} t_k \qquad (A1)$$

Depending on loading, each layer may contain a certain number of transverse cracks which is quantified by the crack density in the k-th layer ρ_k defined as the number of cracks per mm length measured transverse to the crack plane. The crack density in a layer is $\rho_k = 1/(2l_k \sin\theta_k)$, where l_k is the average half distance between cracks in the layer measured on the specimen edge. The dimensionless crack density ρ_{kn} in k-th layer is introduced as

$$\rho_{kn} = t_k \rho_k \qquad (A2)$$

The macroscopic stiffness matrix of the damaged laminate is $[Q]^{LAM}$ and the stiffness of the undamaged laminate is $[Q_0]^{LAM}$. A bar above the matrix and vector entities in the following text indicates layer characteristics in the global coordinate system x, y, z. Classical laminate theory is used to find the stiffness matrix of the undamaged laminate. The kth layer of a symmetric N-layered laminate is characterised by stiffness matrix in the local axes $[Q]$. The fibre orientation angle θ_k defines the stress transformation matrix between

global and local coordinates, and $[T]_k$ is used in CLT to transform stresses, strains and the stiffness matrix. $[\bar{Q}]_k$ is the layer stiffness matrix in global coordinates defined as

$$[\bar{Q}]_k = [T]_k^{-1}[Q]([T]_k^{-1})^{\mathrm{T}} \tag{A3}$$

The undamaged laminate stiffness matrix is calculated as

$$[Q]_0^{LAM} = \frac{1}{h}\sum_{k=1}^{N}[\bar{Q}]_k t_k \tag{A4}$$

Analysing elastic constants of damaged laminate in the framework of CLT, the ply-discount model, is the simplest and most conservative option. The assumption in this model is that as soon as damage appears in a layer the stress in this layer is very low and the layer is not participating in the load sharing. This is formally achieved by taking the elastic constants of the damaged layer equal to zero and calculating the damaged laminate stiffness using (A4). In the version of the ply-discount model used in this paper only the transverse and shear modulus of the layer are zeroed as soon as transverse cracks appear. This version of the ply-discount model is identical to assuming infinite number of transverse cracks in the layer. The predictions of this model are shown in Figures 5 and 7, where experimental axial modulus reduction in the quasi-static test as well as in the cyclic test is also presented.

The ply-discount model predictions are performed in two approximations: (i) assuming that only the 90° layer has cracked (infinite number of cracks); and (ii) assuming that both the 90° and the ±45° layer have cracked. Since cracks were observed in all of these layers, the experimental curves should asymptotically approach to the lowest of the predicted curves. It is clear that the ply-discount model is too conservative.

A much more accurate description of the laminate stiffness reduction with increasing number of cracks in layers can be obtained using the global-local model described in detail in Lundmark and Varna.[33–35] In this model a unique link between global thermo-elastic properties and local stress state characteristics is established. The integral effect of the crack induced stress perturbation is expressed in terms of crack densities, average crack face opening and sliding displacements. The damaged laminate stiffness expressions are as follows

$$[Q]^{LAM} = \left([I] + \sum_{k=1}^{N}\rho_{kn}\frac{t_k}{h}[K]_k[S]_0^{LAM}\right)^{-1}[Q]_0^{LAM} \tag{A5}$$

The $[K]_k$ matrix-function for a layer with index k is defined as

$$[K]_k = \frac{2}{E_2}[\bar{Q}]_k[T]_k^T\begin{bmatrix} 0 & 0 & 0 \\ 0 & u_{2an}^k & 0 \\ 0 & 0 & \dfrac{E_2}{G_{12}}u_{1an}^k \end{bmatrix}[T]_K[\bar{Q}]_k \tag{A6}$$

These matrix expressions for thermo-elastic properties contain elastic ply properties, details of laminate lay-up and dimensionless density of cracks in each layer. In addition, the influence of each damage entity is represented by the 3×3 displacement matrix in (A6) which contains the normalised average crack opening displacement (COD), u_{2an}^k and normalised average crack sliding displacement (CSD), u_{1an}^k of the crack surfaces in k-th layer. In (A5) $[I]$ is the identity matrix. Expressions for u_{2an}^k and u_{1an}^k calculation are obtained fitting an extensive FEM based parametric analysis. The expression for u_{2an} is

$$u_{2an} = A + B\left(\frac{E_2}{E_x^s}\right)^n \tag{A7}$$

In (A7), E_x^s is the Young's modulus of the layer supporting the cracked layer in the transverse direction of the damaged layer. For a crack in an internal layer:

$$A = 0.52 \quad B = 0.308 + 0.165\left(\frac{t_{90}}{2t_s} - 1\right)$$
$$n = 0.0307\left(\frac{t_{90}}{2t_s}\right)^2 - 0.0626\left(\frac{t_{90}}{2t_s}\right) + 0.704 \tag{A8}$$

In (A8), t_s is thickness of the adjacent support layer and t_{90} is thickness of the cracked layer. For a crack in a surface layer:

$$A = 1.2 \quad B = 0.594 + 0.190\left(2\frac{t_{90}}{t_s} - 1\right)$$
$$n = -0.523\left(\frac{t_{90}}{t_s}\right)^2 + 0.887\left(\frac{t_{90}}{t_s}\right) + 0.258 \tag{A9}$$

The crack face sliding displacement u_{1an}, also follows a power law:

$$u_{1an} = A + B\left(\frac{G_{12}}{G_{xy}^s}\right)^n \tag{A10}$$

In (A10), G_{xy}^s is the in-plane shear modulus of the support layer in the coordinate system of the damaged layer. For cracks in an internal layer:

$$A = 0.3 \quad B = 0.066 + 0.054\frac{t_{90}}{2t_{\mathrm{s}}} \quad n = 0.82 \quad \text{(A11)}$$

For cracks in a surface layer:

$$A = 0.6 \quad B = 0.134 + 0.105\frac{t_{90}}{t_{\mathrm{s}}/2} \quad n = 0.82 \quad \text{(A12)}$$

Expressions (A7) to (A9) and (A10) to (A12) show that the normalised average COD and CSD are larger for less stiff surrounding layers and they approach to a certain asymptotic value with increasing support layer and cracked layer stiffness ratio. For thicker support layers the COD and CSD are smaller. This effect of neighbouring layers on the crack face displacements is called the constraint effect.

The presented expressions (A7)–(A12) are valid for relatively low crack densities in layers (so called non-interactive crack region) corresponding to the experimental case in this study. For high crack densities the interaction between cracks reduces the values and the stiffness reduction slows down.[35,38,44,45]